Frequency Response of MV Voltage Transformer Under Actual Waveforms

Frequency Response of MV Voltage Transformer under Actual Waveforms

G. Crotti, D. Gallo, *Member, IEEE*, D. Giordano, C. Landi, *Member, IEEE*,
M. Luiso *Member, IEEE* and M. Modarres.

***Abstract*— A set-up for the measurement of the frequency response of voltage measurement transformers under actual waveform conditions is presented. It is based on a two steps procedure that makes use of high voltage gas insulated capacitors and a digital bridge. It allows calibrations using distorted waveforms, with a fundamental tone at medium voltage level and superimposed harmonics up to 20% and 15 kHz. Combined standard uncertainty in the measurement of the voltage transformer error is estimated 200 µV/V for the ratio error and 300 µrad for the phase displacement up to 10 kHz. First applications to the measurement of the frequency response of voltage transformers with different rated primary voltages up to 50 kV are presented.**

***Index Terms*— Calibration, voltage transformers, medium voltage, frequency response, measurement uncertainty.**

I. Introduction

The increase of disturbances and quality deterioration of the transferred power in transmission and distribution grids call for extended performances of the measurement systems employed for metering, protection coordination and monitoring of grid stability and power quality [1]-[10]. Measurement instrument transformers are installed at both high voltage (HV) and medium voltage (MV) level to scale the grid voltage and current to values compatible with the input of the measuring instruments. When used in the measurement of the grid power and/or of its quality, they are required to accurately operate over a wide range of amplitudes and frequencies, which may extend beyond the 50th harmonic [11]-[12]. Installed inductive measurement voltage transformers (VT) are generally calibrated at the rated voltage at power frequency only. Their frequency characterization, if performed, is carried out at voltages which are usually more than one order of magnitude lower than the rated ones, without considering the non-linearity of the device. Measured VT behaviors show that non negligible variations can be found when comparing the values measured at low voltage with those obtained at some kilovolt [14]. There is then a need for characterized and traceable methods to assess the VT performances under actual conditions in a frequency range up to several kilohertz. Moreover, an accurate determination of the complex VT frequency response over an extended range up to the first resonances can allow the implementation of real-time correction procedures for VTs with unsatisfactory frequency response [15].

Solutions proposed for the frequency calibration at MV are generally based on the use of an arbitrary waveform generator (AWG), which can be connected to an amplifier, that feeds the low voltage winding of a step-up transformer [16]. Because of the distortion and variability of the supplied MV signal, a reference transducer, such as a MV divider, is needed to accurately measure the components of the applied signal over the frequency range of interest.

An alternative method for the measurement of the ratio and phase errors of MV measurement transformers in the frequency range up to 15 kHz, has been introduced in [17]. It consists of a two-step procedure based on the use of HV capacitors and a digital current comparator. It is intended for the frequency characterization at full rated voltage of VTs with primary voltage up to $36/\sqrt{3}$ kV (fundamental tone), employing a frequency sweep of a single harmonic tone, whose amplitude can be selected up to 20 % of the fundamental tone. In the paper, the previously introduced method [17] is refined, characterized and experimented in the measurement of the complex frequency response of VTs. In the following, a brief description of the measurement set-up is given, the analysis of the uncertainty contribution is performed and results of its application to the evaluation of the ratio and phase errors of commercial VTs from a few hertz up to 15 kHz are shown and discussed.

II. Calibration Procedure

The developed method for the frequency calibration of MV VTs is a modified extension of the absolute method commonly implemented in the National Metrology Laboratories for the calibration at power frequency of standard transformers, with uncertainties ranging from a few microvolts/volt (microradiants) to 100 µV/V (100 µrad) for the ratio (phase) error [18], **Error! Reference source not found.**. In the next

The research leading to the results here described is part of the European Metrology Research Program (EMRP), ENG52 Smart Grid II project. The EMRP is jointly funded by the EMRP participating countries within EURAMET and the European Union.

G. Crotti and D. Giordano are with the Istituto Nazionale di Ricerca Metrologica, Torino, Italy (email: g.crotti@inrim.it, d.giordano@inrim.it.

M. Modarres is with the Dipartimento Energia del Politecnico di Torino, Italy (e-mail:mohammad.modarres@polito.it).

D. Gallo, C. Landi and M. Luiso are with the Department of Industrial and Information Engineering, University of Campania "Luigi Vanvitelli", Aversa (CE), Italy (e:mail: daniele.gallo@unina2.it, carmine.landi@unina2.it, mario.luiso@unina2.it).

ubsections, the measurement procedure and the circuital implementation are detailed.

A. Measurement method

The calibration is performed by a two step procedure using two HV gas insulated capacitors C_1 and C_2 and a digital current comparator. In the first step (*a*), the two high voltage capacitors are both connected to the MV. The supply voltage (sinusoidal or distorted) is generated by an arbitrary waveform generator coupled with a MV power amplifier. The currents i_{C1} and i_{C2}, which flow into capacitors C_1 and C_2 are converted into the voltages V_{CH1} and V_{CH2} by transimpedance amplifiers with feedback resistors R_{CH1} and R_{CH2} [20]. The ratio $k_{a,h}$ and phase displacement $\Delta\varphi_{a,h}$ of each harmonic component *h* of V_{CH1} and V_{CH2} can be evaluated by making use of a two-channel digitizer based system as:

$$\begin{cases} k_{a,h} = \dfrac{|V_{CH1}|_{a,h}}{|V_{CH2}|_{a,h}} \\ \Delta\varphi_{a,h} = \varphi_{V_{CH2},h} - \varphi_{V_{CH1},h} \end{cases} \quad (1)$$

with

$$k_{a,h} = \frac{|V_{CH1}|_{a,h}}{|V_{CH2}|_{a,h}} = \frac{R_{CH1}}{R_{CH2}} \cdot \frac{C_1}{C_2} \quad (2)$$

where $|V_{CH1①,h}|$ and $|V_{CH2①,h}|$ are the measured voltage amplitudes of the *h*-th-harmonic component at measurement step a) and $\varphi_{VCH1①,h}$ and $\varphi_{VCH2①,h}$ are the corresponding measured phases. In the second step (b), the VT under calibration is inserted between the MV connection and capacitor C_2, according to the circuit shown in Fig.1. The ratio $k_{b,h}$ and phase displacement $\Delta\varphi_{b,h}$ of V_{CH1} and V_{CH2} are then expressed as:

$$\begin{cases} k_{b,h} = \dfrac{|V_{CH1}|_{b,h}}{|V_{CH2}|_{b,h}} = \dfrac{R_{CH1}}{R_{CH2}} \cdot \dfrac{C_1}{C_2} \cdot \dfrac{V_{H,h}}{V_{L,h}} = \\ \Delta\varphi_{b,h} = \varphi_{V_{CH2b,h}} - \varphi_{V_{CH1b,h}} \end{cases} \quad (3)$$

where $V_{H,h}$ and $V_{L,h}$ are the *h*-th component of the applied voltage V_H and of the VT output voltage V_L respectively.

Under the assumption of negligible variation of capacitor C_2 between step a) and b), the ratio error $\varepsilon_{VT,h}$ and the phase error $\varphi_{VT,h}$ of the VT under calibration, related to the measurement of *h*-component and defined according to [21], are expressed as:

$$\varepsilon_{VT,h} = \left(k_r \frac{k_{a,h}}{k_{b,h}} - 1 \right) \qquad \varphi_{VT,h} = \Delta\varphi_{a,h} - \Delta\varphi_{b,h} \quad (4)$$

and the VT complex transfer function $G_{VT(f)}$ at frequency $f=h\cdot f_0$ is:

$$G_{VT(f)} \cdot e^{i\varphi_{VT}(f)} = \left(k_r \frac{(V_{CH1}/V_{CH2})_{a,h}}{(V_{CH1}/V_{CH2})_{b,h}} \right) \quad (5)$$

The use of this two-step procedure, with respect to other methods, such as the one that makes use of a current comparator based transimpedance amplifier with a low-loss feed-back capacitor, coupled with a HV capacitor connected to the input [22, 23], is adopted to exploit the amplification of the harmonic component due to the differentiating circuit, to get accurate measurement of high order low amplitude harmonics.

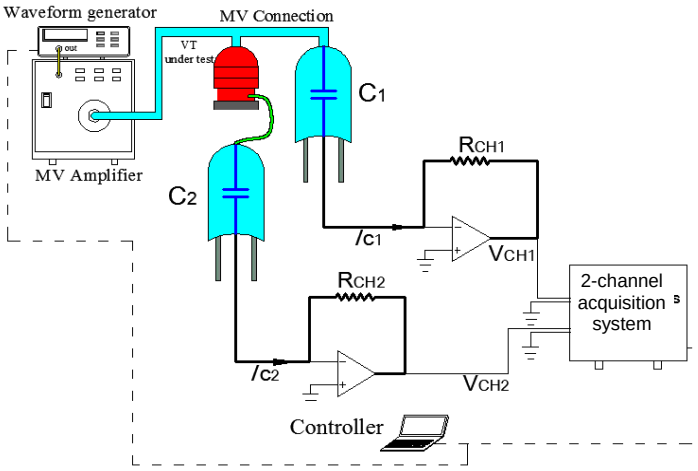

Fig. 1. Generation and measurement circuit for the VT frequency calibration (step b)

B. Supply and measurement circuit

With reference to Fig 1, compressed-gas HV standard capacitors are used, which are routinely employed for power frequency calibrations of VTs. C_1 is a 103.5 pF, 250 kV capacitor, whereas C_2 is chosen between a 1.046 nF, 60 kV and a 10.106 nF, 15 kV capacitor, depending on the measurement conditions.

As to the transimpedance amplifier, the operational amplifiers OPA606 [24] with maximum supply voltage of 15 V are considered, so that, the maximum output voltage, V_{CH}_max, is 8 V_{rms}. Main specifications of the OPA606 are bandwidth of 13 MHz, slew rate of 35 V/μs, offset current of 1 pA, distortion of 0.0035 % at 10 kHz. As to R_{CH1} and R_{CH2}, 900 Ω, 0.5 W feedback resistors are used. Feedback capacitors C_{CH1} and C_{CH2}, in parallel to R_{CH1} and R_{CH2} (not shown in Fig. 1), with rated capacitance equal to 2 nF and operating voltage up to 3 kV, have been introduced to reduce noise and the effects of stray capacitances on phase measurement.

To generate sinusoidal or distorted voltage signal, an arbitrary waveform generator board (NI 5422), equipped with a software-selectable 7-pole analog elliptical filter for image suppression, is used. The low voltage signal is then amplified by a MV power amplifier [25] (30 kV_{peak}, 20 mA_{peak}, 2.5 kHz for large signals, 30 kHz for small signals) producing the MV waveform. The frequency sweep is carried out by applying a distorted waveform composed of two tones: the fundamental one at rated voltage and a low voltage tone with variable frequency and phase angle. For this application, the particular case of a harmonic tone with zero phase is considered, but this does not constitute a limit of the utilized setup. The V_{CH1} and V_{CH2} signals are digitized by a NI 9239 10 V, 24 bit, 50 kHz board, equipped with a 24.56 kHz anti-aliasing filter, and the fundamental and harmonic tone amplitude and phase are

estimated as described in the next subsection. The use of the 10 nF capacitor can be preferred for C_2, especially in presence of harmonic frequencies of the order of a few hundreds of hertz, because of the higher amplitude of the harmonic current to be measured. On the other hand, since same R_{CH2} is used in both steps *a* and *b*, the applied 50 Hz high voltage has to be limited in step *a*, in order to avoid saturation of the digitizer considering the C_2 value.

C. Identification of the spectral components

The reference signal is made of the sum of two contributions: the first, s_F, is an AC sinusoidal signal at fundamental frequency f_1 and the second, s_H, is a sinusoidal signal at the *h*-th harmonic frequency of f_1. The signal *s(k)* obtained after A/D conversion can be written as:

$$s(k) = s_F(k) + s_H(k) = \\ = A_1 \sin\left(2\pi f_1 \frac{k}{f_S} + \varphi_1\right) + A_h \sin\left(h \cdot (2\pi f_1) \cdot \frac{k}{f_S} + \varphi_n\right) \quad (6)$$

where f_s is the sampling frequency, *h* is the harmonic order, A_1, A_h and φ_1, φ_h are the amplitude and phase angle of the fundamental and *h*-th harmonic component respectively.

In principle, in order to obtain exact values for *h*, A_1, A_h, φ_1 and φ_h, a synchronized spectral analysis should be performed, thus a time window exactly synchronized with fundamental frequency should be processed by Discrete Fourier Transform (DFT). This is possible when there is an accurate synchronization between power frequency f_1 and sampling frequency f_s, that is when the generation and the acquisition devices share the same clock, provided by external synchronization devices. In fact, a not exactly synchronized analysis gives inaccurate results due to the spectral leakage on the estimations of both the components. In a general case, anyway, the reference signal can be composed by two spectral components whose frequencies are not in an integer ratio (e.g. the case of an inter-harmonic in power system quantities). In this case, an accurate synchronization is possible for only one of the two tones. Therefore, here, the problem of identifying the parameters of the two tones is solved by applying a digital signal processing technique [26] more complex than a simple DFT; in this way, the necessity of synchronization devices is overcome, thus making a simpler measurement set-up, and improving accuracy. The flow chart of the signal processing technique, that solves the discussed synchronization problems without additional hardware, is shown in Fig. 2.

After step 1 of signal elaboration (Fig.2), it is:

$$s_w(k) = s(k) \cdot w'(k) \qquad \text{with k=0,1,....,L-1} \quad (7)$$

being *w'* the adopted 1st stage window of length $T_W = L/f_S$.

In step 2, the spectral components of interest are individually evaluated or a whole DFT is calculated.

In step 3, an accurate estimation of the frequency f_1, of the amplitude A_1 and phase angle $\hat{\varphi}_1$ of the fundamental component is obtained by means of opportune interpolation techniques of the desynchronized spectral components calculated at step 2 [23]. The estimated fundamental component (6) is then numerically generated:

$$\hat{s}_F(k) = \hat{A}_1 \sin\left(2\pi \hat{f}_1 \cdot \frac{k}{f_S} + \hat{\varphi}_1\right) \quad (8)$$

In step 4, the contribution (3) can be obtained from the original signal, i.e. in the time domain, obtaining an estimation of the harmonic contribution (4):

$$\hat{s}_H(k) = s(k) - \hat{s}_F(k) \qquad \text{with} \quad k = 0,1,.....,L-1. \quad (9)$$

A suitable window *w''*, which can in general differ from previous *w'*, is then used to reduce the residual harmonic leakage problems:

$$\hat{s}^I_{w''}(k) = \hat{s}^I(k) \cdot w''(k) \qquad \text{with} \quad k = 0,1,.....,L-1 \quad (10)$$

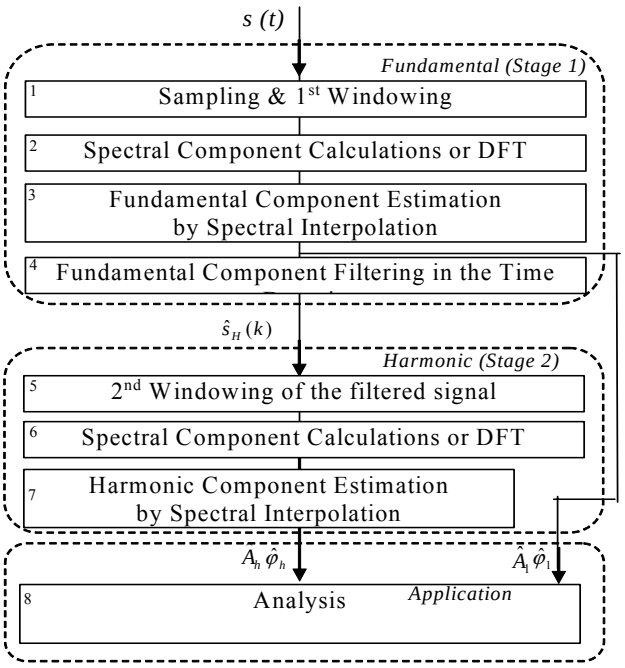

Fig. 2. Flow-chart of the desynchronized processing technique.

In step 6, the windowed signal (10) is subjected to a second spectral analysis, so that spectral components of interest are individually evaluated or a whole DFT is calculated. From these values, it is possible (step 7) to estimate the amplitude, the frequency and the phase angle of the harmonic component performing further spectral interpolations.

Finally, it is worthwhile underlining that steps 5 and 6 in Fig. 2 can be skipped performing the harmonic filtering in the frequency domain.

III. Uncertainty analysis

Expressions (4) and (5) are valid under a number of simplifying assumptions, which have to be valid with reference to step a) and b) measurement conditions. They include current linearity of resistor R_{CH2}, voltage dependence of capacitor C_2, negligible errors of the data acquisition and processing system. Moreover, a null loading effect of C_2 on the VT response is assumed. An accurate estimate of the

contributions of all the possible uncertainty sources has then to be performed to evaluate the calibration method performances in terms of achievable uncertainty.

A. Circuital component

To evaluated its stray parameters, measurements of the complex impedance of R_{CH2} versus frequency were carried out with an impedance analyzer, covering the frequency range from 40 Hz to 110 MHz. The obtained results show that its reactance is negligible up to some hundreds kilohertz, being the resonance frequency at several megahertz.

The current heating effect on R_{CH2} is estimated by measuring the resistance variations when currents of the same order of magnitude as those expected during the two steps of the calibration process flow through R_{CH2}. Assuming applied voltages from 1 kV_{RMS} to 30 kV_{RMS}, tests were carried out with DC and AC currents from a few microampere up to 6 mA.

As regards the amplifier, a non-linearity effect of channel 2 should be considered. The contribution to the total uncertainty budget is obtained from the component specification [24].

The voltage dependence of both C_2=1 nF and C_2=10 nF capacitors are estimated by comparison with a 700 kV capacitor by measuring the capacitance variations at increasing voltages up to 60 kV and 11 kV respectively. As an example, the 1 nF capacitor measured variation with respect to the 1 kV value is 24 µF/F at 20 kV (1.5 µrad for the loss angle), which reduces to 5 µF/F at 10 kV (0.5 µrad). For the non-commercial 10 nF capacitor, significantly larger variations are found at 11 kV with respect to the 1 kV (336 µF/F and 42.5 µrad). For such non-commercial high capacitance value-high voltage capacitor, these variations can be explained considering the high electrodynamic effects. Corrections for the C_2 voltage dependence are then introduced.

Standard uncertainty contributions associated with C_{CH2} variation between steps *a)* and *b*) are introduced as a function of the frequency, starting from the capacitor specifications. They result negligible for frequencies up to 1 kHz (less than 0.01 µV/V for the ratio error and 1 µrad for the phase) and increase up to 0.75 µV/V and 6.3 µrad at 10 kHz).

All measurements described in the following sections were carried out in the high voltage INRIM laboratory, which is temperature controlled. Temperature variations experienced by the HV and feedback capacitors during the two step measurements are well within 0.25 K. The consequent relative variation of HV capacitances are within ± 4 µF/F for capacitor C_1 (temperature coefficient 17 µF/F/K) and ± 5 µF/F for capacitors C_2 (temperature coefficient 20 µF/F/K). Similar variations are conservatively assumed for the C_1 and C_2 losses.

For the feedback capacitors, their temperature coefficient is (100 µF/F/K). However, taking into account that, in each step, the same capacitors are used in the two branches of the circuits and the considered temperature variation (0.25 K), their relative variation due to temperature is expected to be to be within the ppm and for this reason is assumed negligible. As to the VT loading effect of C_2, typical values of commercial MV VT burden are in the order of some tens of volt-ampere. With the adopted capacitance values (1 nF or 10 nF), the contribution to the burden, at 50 Hz, is in the order of 1 µVA/VA and can be disregarded.

With the increase of the frequency, the C_2 loading effect depends on the values of the internal VT stray capacitances (capacitances between winding turns, between turns and ground), which in turn depend on the VT rated voltage and winding arrangements. Consequently, the capacitive burden effect cannot be given a priori. Moreover, in the on-site conditions, additional capacitive load can be introduced e.g. by the connection cables. As a general consideration, similar to the VT 50 Hz calibration, where the test burden is normally the rated one defined by the manufacturer, a "capacitive rated burden" could be defined when the VT has to be frequency characterised. The uncertainty on its value would then contribute to the uncertainty associated with the ratio and phase error in the frequency domain. To estimate this uncertainty, a comparison between the ratio and phase errors of the 20/√3 kV : 100/3 V VT measured both with a 1 nF and a 10 nF capacitance has been performed up to 3 kHz. The test has provided a deviation, under 9 nF capacitance variation, within 200 µV/V (200 µrad) over the considered frequency range. Assuming an uncertainty on the capacitance value of 25 µF/F, the variation on the measured VT ratio error at 3 kHz is of 0.01 µV/V, which can be disregarded. Similar consideration can be done for the uncertainty of the phase error.

As to the digitizers, the ratio and phase errors, introduced when increasing signals of different amplitudes are acquired, are evaluated by imposing input signals with known ratio by means of a calibrated inductive divider and, at increasing frequencies by a phase standard generator [27].

B. Spectral component identification

The accuracy of the technique used for the identification of the spectral components is investigated by applying distorted test signals with superimposed noise. In all the simulations, sampling frequency is set to 50 kHz and 50000 samples are analyzed.

In the first test, a signal composed by a fundamental tone with frequency of 50.1 Hz, amplitude of 1 V, phase of 0 rad and a third harmonic tone with amplitude equal to 20 % of the fundamental tone and phase of 0 rad is analyzed. Sampling frequency and signal frequency are not synchronized.

White noise is added to the signal, making its Signal-to-Noise Ratio (SNR) variable. Thirty iterations for every SNR value are performed. Fig. 3 shows the standard deviation of the mean deviation Δf_F between the computed fundamental frequency and the imposed one versus the SNR. As can be seen, even in harsh condition, that is desynchronization and very low SNR (20 dB), the standard deviation is lower than 1 mHz. For a SNR higher than 60 dB, that is a typical value for calibration applications, the standard deviation reduces to less than 10 µHz.

In the second simulation the effect of the harmonic frequency on the performance of the proposed technique is analyzed. Therefore a signal composed of a fundamental tone with frequency 50.1 Hz, amplitude of 1 V, phase of 0 rad and a harmonic tone with variable order from 2 to 296 (i.e. up to

about a frequency of 15 kHz), amplitude of 20 % of the fundamental tone and phase of 0 rad is analyzed. For sake of brevity only figures related to phase estimation are shown. White noise is added to the signal to have a SNR of 60 dB. Figure 4 shows the mean $\Delta\varphi_F$ of the fundamental phase deviation from to the reference value and $\Delta\varphi_F$ its standard deviation u_A.

Figure 5 shows the same quantities, but with reference to the harmonic phase deviation $\Delta\varphi_H$. As can be seen, even with desynchronization between fundamental and sampling frequencies, the 2 u_A range is always lower than 20 µrad and 100 µrad for the fundamental and the harmonic phase, respectively. As to the evaluation of the fundamental and superimposed harmonic amplitude under the same test conditions, the 2 u_A range is always lower than 2.0 µV/V and 1.0 µV/V for the fundamental and the harmonic amplitude respectively.

In the third test, the effect of the jitter on the sampling interval is evaluated. A sinusoidal signal, with frequency 50 Hz, amplitude 1 V, phase 0 rad, is considered and white noise is added to the sampling interval value.

Fig. 6 shows the standard deviation of the mean deviation Δf_F between the computed fundamental frequency and the imposed one versus the sampling interval jitter, expressed in picoseconds.

With typical values for jitter in calibration applications, that are lower than 100 ps, the standard deviation is lower than 50 µHz.

C. Uncertainty evaluation

On the basis of the results obtained from the measurements performed as described in the previous section, an estimate of the measurement uncertainty has been carried out.

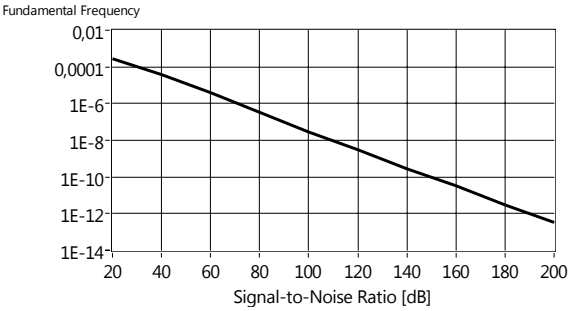

Fig. 3. Standard deviation of the mean fundamental frequency (50.1 Hz) deviation Δf_F from the reference value vs. Signal-to-Noise Ratio.

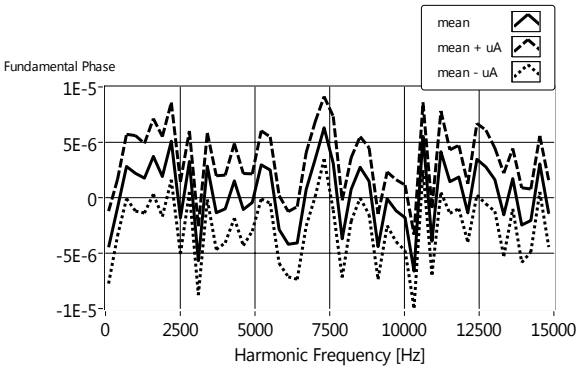

Fig. 4. Fundamental phase deviation ($\Delta\varphi_F$, $\Delta\varphi_F + u_A$, $\Delta\varphi_F - u_A$) vs. harmonic frequency.

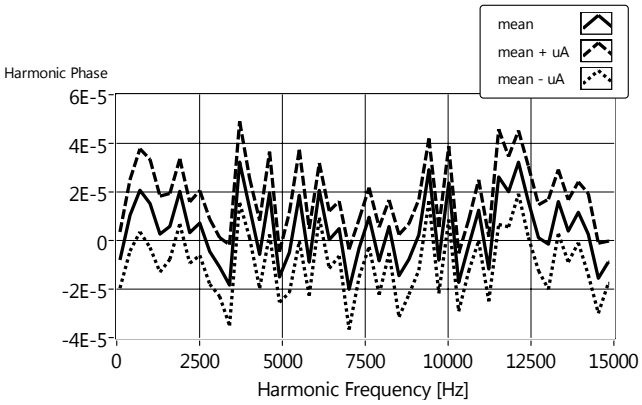

Fig. 5. Harmonic phase deviation ($\Delta\varphi_H$, $\Delta\varphi_H + u_A$, $\Delta\varphi_H - u_A$) vs. harmonic frequency

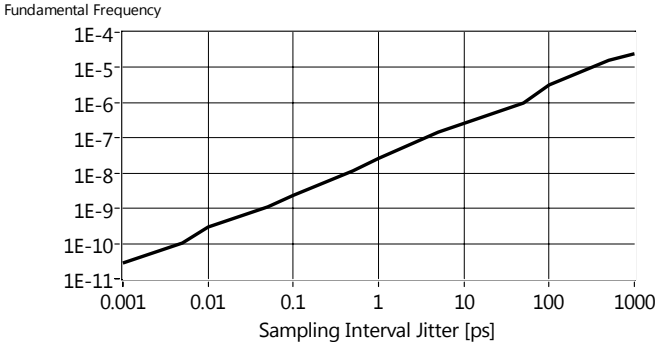

Fig. 6. Standard deviation of the mean fundamental frequency (50 Hz) deviation Δf_F from the reference value vs. Sampling Interval Jitter.

Table I shows the uncertainty budget relevant to the frequency calibration of a 20/√3 kV/100/3 V VT at rated voltage (11 kV_{RMS}), with reference to the measurement of a distorted signal with superimposed 20 % to 1 % harmonics up to 10 kHz. The standard uncertainty component due to the C_2 voltage dependence is the uncertainty of the introduced correction factor, obtained as described in section III A with reference to the applied rated voltage of 11 kV.

TABLE I - UNCERTAINTY BUDGET (UP TO 10 KHZ)

Quantity/Influence factor	Standard uncertainty contribution	
	Ratio error (µV/V)	Phase error (µrad)

R_{CH2} non linearity:	5	2
C_2 voltage dependence:	3	3
C_1 temperature stability	2.3	2
C_2 temperature stability	2.9	2.9
C_{CH2} 2-steps variation	<1	from 0.03 to 6.3
Amplifier non linearity	20	20
VT loading	1 (200*)	1 (200*)
Digitizers, repeatability and identification algorithm	200	300

(*) f= 3kHz, C_2=10 nF, assumed rated capacitive load 1 nF).

Conservatively assuming a quadratic increase of the C_2 loading effect with frequency, the uncertainty component, due to the C_2 loading effect, estimated as described in section III A, is negligible up to 10 kHz, provided that measurements are performed with a known rated load. If a rated load is not defined, a more conservative approach can be adopted, particularly in the case of the use of the 10 nF capacitance, to include in the uncertainty budget the uncertainty component obtained considering the variation with respect to the 1 nF load. Such values are indicated in Table I within the brackets for a frequency of 3 kHz. As can be seen, the predominant uncertainty contribution is the one relevant to the digitizer and identification algorithm and to the reading repeatability.

IV. Validation of the Measurement Method

A first validation of the method has been carried out by comparing the results obtained for the fundamental tone, when a VT frequency characterization under distorted waveform (two tone frequency sweep: fundamental with a superimposed harmonic) is carried out, with those obtained measuring the VT ratio and phase with the INRIM reference set-up for 50 Hz calibration (measurement standard uncertainty: ratio error 25 µV/V, phase error 25 µrad). The fundamental (60 Hz) phase errors of a VT with rated primary voltage 20/√3 kV and output voltage 100/3 V, measured in tests carried out with increasing frequency superimposed harmonic from 180 Hz to 3 kHz are shown in Fig. 7. Deviations from the reference 50 Hz value (continuous bold red line), measured by the INRIM reference set-up, are all well within 22 µrad. Similar results are found for the ratio error deviations.

V. Measurement of VTs Frequency Response

As a first application, the proposed method is experimented in the frequency calibration of three different measurement voltage transformers with rated primary voltage 11/√3 kV VT0), 20/√3 kV (VT1) and 50 kV (VT_REF). The laboratory layout is shown in Fig. 8. Table II shows the rated characteristics of the considered voltage transformers.

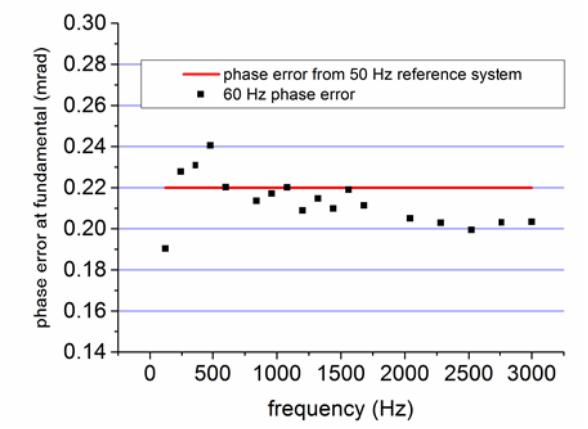

Fig. 7. VT1 phase error at fundamental frequency (60 Hz) obtained by the two tones measured signals versus the harminc tone frequency (dots), data are compared with the VT1 50 Hz phase error measured by the INRIM power frequency reference calibration system. (continous bold red line).

TABLE II - RATED CHARACTERISTICS OF THE INVESTIGATED VTS

	U_p (kV)	U_s (V)	*Rated Burden*	*Accuracy class*
VT0	11√3	110/√3	50 VA, 0.8 ind.	0.5 - 3P
VT1	20√3	100/3	50 VA, 0.8 ind	0.5 - 3P
VT_REF	50	100	0 VA – 20 VA, 0.8 ind.	0.1

TABLE III – VT TEST CONDITIONS

	F_{fund} (Hz)	V_{fund} (kV)	Harmonic amplitudes (% of the fundamental)		
VT0	50	3	f_H = 2 – 10	f_H = 11 - 28	f_H = 29 – 300
			20 %	5 %	1 % - 0.2 %
VT1	60	11	f_H = 2 – 10	f_H = 11 - 28	f_H = 29 – 172
			20 %	5 %	1 % - 0.2 %
VT_REF	60	22	f_H = 2 – 24	f_H = 25 - 88	
			20 %	2 %	

Fig. 8. Circuital layout for the calibration of the MV VTs.

The frequency analysis of the three VTs is performed by applying a distorted 2-tone waveform, whose components are summarized in Table III. Moreover, for one of the three VTs, a single tone frequency sweep at low voltage is carried out.

For each considered VT, the measurements are carried out up to several kilohertz to identify at least the first two amplitude resonances. For the VT with the lower rated voltage (VT0), the first resonance frequency is detected at 9.3 kHz. As to VT1, measurements are performed at rated primary voltage both with rated burden and with null imposed burden. In addition, a single tone frequency sweep at low voltage is carried out. Fig. 9 a) compares the measured ratio and phase errors up to 3 kHz for VT1. The 50 Hz ratio error, measured with the INRIM power frequency reference system is also indicated (yellow dot). For both VT0 and VT1, characterisation is performed with C_2=10 nF.

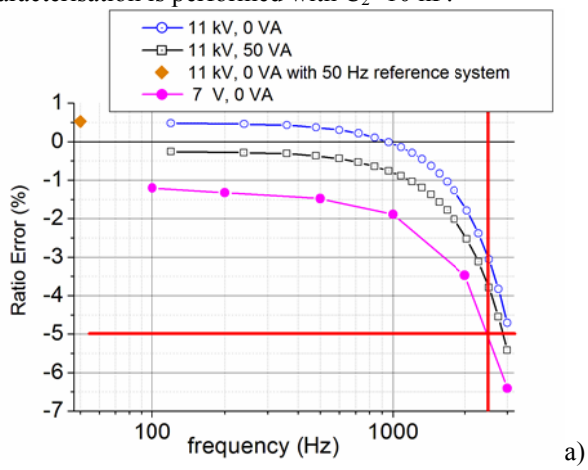

Fig. 9. Ratio (a) and phase (b) error of VT1 with and without the 50 VA rated burden from 120 Hz to 3 kHz. Yellow dot in graph (a) ratio error estimated with the 50 Hz reference calibration system , the frequency sweep obtained by applying 7 V and the accuracy limit up to 2.5 kHz are also shown (continous bold red line).

Deviations of about 2 % and up to 1 mrad are found between the MV waveform data and those measured in the low voltage characterization. It must be noted that the 2.5 kHz ratio error value measured at MV voltage is clearly compliant with the limits indicated by the relevant standard [12] for the ratio and phase errors of VTs used for harmonic evaluation in power quality measurements. On the contrary, the low voltage value is practically coincident with the prescribed limits.

The scale factor, defined as the ratio of the applied voltage to the output voltage, and phase errors measured on the same VT up to 10 kHz are shown in Fig. 10. A first resonance peak is detected for the ratio error at 5.65 kHz, whereas a second one is found at about 6 kHz. Further resonances were evidenced up to the maximum investigated range (15 kHz, not shown).

As to VT_REF, with a significantly higher rated voltage (50 kV), frequency analysis, carried out with C_2 = 1 nF, highlights the presence of a first resonance already at 2 kHz (Fig. 11). As clearly evidenced by the comparison with the red lines (continuous line), which corresponds to the standard indicated accuracy limits, the use of this VT in PQ measurements is limited at frequencies lower than 1 kHz.

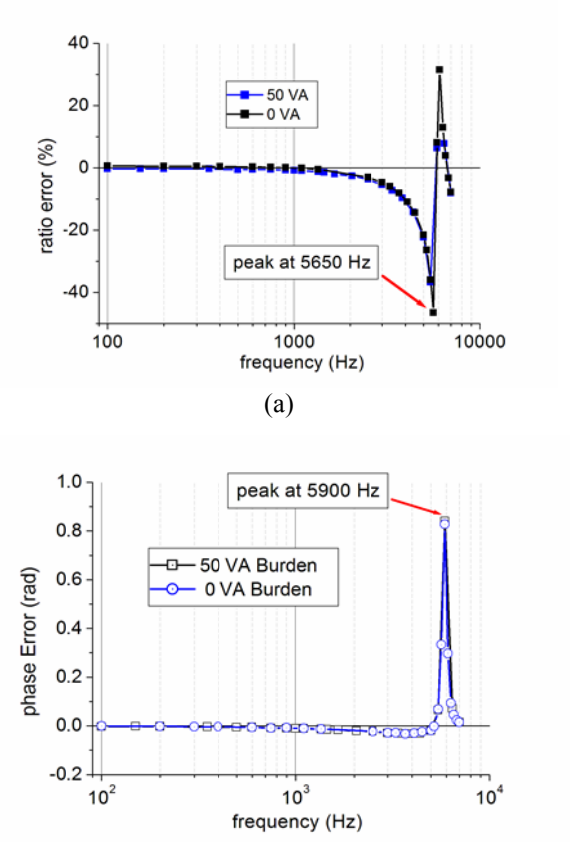

Fig. 10. Ratio (a) and phase (b) error of VT2 with and without the 50 VA rated burden from 100 Hz to 7 kHz. The resonance condition is highlighted in graph (a).

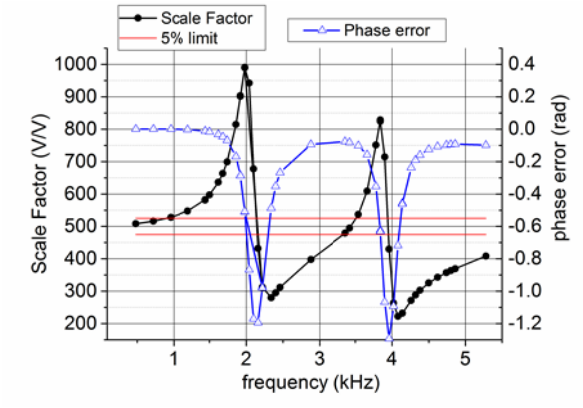

Fig. 11. Scale Factor and Phase error of VT_REF with 0 VA burden.

VI. Conclusion

A method for the accurate ratio and phase frequency calibration of MV inductive voltage transformers under distorted MV voltages has been developed and experimented in the frequency characterization of MV commercial VTs. Depending on the primary rated voltages, the frequency response analysis can be extended up to 15 kHz. Best standard combined uncertainty in the measurement of ratio error and phase displacement has been estimated to be 200 µV/V for the ratio error and 300 µrad for the phase up to 10 kHz. As regards the applied primary voltages, the calibration arrangement is presently limited to 22 kV. Extension to higher voltages will be made possible by the use of power amplifiers with higher generation capabilities and/or the introduction of suitable step up transformers. Improvement of the method will be obtained by the use of selectable gains for the trans-impedance amplifier to optimize the match of the output voltage signals with the input characteristics of the digitizers.

It is worthwhile noting that with the presented solution, the obtained uncertainty, up to several kilohertz, are about two order of magnitudes lower than the accuracy limits specified for the VT to be characterized in the frequency range up to 50th harmonic and over.

First measurements carried out on commercial VTs with rated primary voltages from 11/√3 kV to 50 kV, show some interesting results. First of all, variations of the order of some percent are found with respect to the frequency characterization carried out at low voltage. Moreover, the presented method allows the detection at least of the first VT resonances, phenomena that can have detrimental effect on PQ measurements. First obtained results show that compliance with the error limits prescribed by the relevant standard for VTs used in PQ measurements is found for the 11 kV/√3 VT even beyond the 50th harmonic, and for the 20 kV/√3 VT compliance up to 2.5 kHz. A more critical situation is found in the case of the 50 kV VT, whose first resonance frequency is detected at 2 kHz.

As a next step, an extended measurement campaign on VTs of different manufacturers and/or rated primary voltage will be carried out to confirm the results obtained and provide recommendations about the best approach for the measurement of frequency response of instrument voltage transformers.

References

[1] P. K. Ray, S. R. Mohanty, N. Kishor, "Classification of Power Quality Disturbances Due to Environmental Characteristics in Distributed Generation System", *IEEE Trans. Sustain. Energy*, vol. 4, no. 2, pp. 302–313, Apr. 2013.

[1] P. Sorensen, "Power quality issues on wind power installations in Denmark", *Proc. IEEE Power Engineering Society General Meeting*, pp. 1-6, Jun. 2007.

[2] S. A. Papathanassiou and F. Santjer, "Power-quality measurements in an autonomous island grid with high wind penetration", *IEEE Trans. Power Del*., vol. 21, no. 1, pp. 218-224, Jan., 2006.

[3] R. W. D. Doncker, C. Meyer, R. U. Lenke and F. Mura. "Power electronics for future utility applications", Proc. 7th Int. Conf., Power Electronics and Drive Systems, pp. K-1-K-8, 2007.

[4] D. Gallo, C. Landi, N. Pasquino and N. Polese, "A new methodological approach to quality assurance of energy meters under non-sinusoidal conditions", *IEEE Trans. Instrum. Meas*., vol. 56, no. 5, pp. 1694-1702, May, 2007.

[5] *IEEE Standard for Synchrophasor Measurements for Power Systems*, C37.118.1-2011 and amendment 2013.

[6] *IEEE Guide for Synchronization, Calibration, Testing, and Installation of Phasor Measurement Units (PMUs) for Power System Protection and Control*, C37.242-2013.

[7] *Electromagnetic Compatibility (EMC)—Part 4–30: Testing and Measurement Techniques—Power Quality Measurement Methods*, IEC 61000-4-30, 2008.

[8] *Electromagnetic Compatibility (EMC)—Part 4–7: Testing and Measurement Techniques—General Guide on Harmonics and Interharmonics Measurements and Instrumentation, for Power Supply Systems and Equipment Connected Thereto*, IEC 61000-4-7, 2009.

[9] J. Luszcz and R. Smolenski, "Voltage harmonic distortion measurement issue in smart-grid distribution system," in *Proc. Asia-Pacific Symp. Electromagn. Compat. (APEMC)*, May 2012, pp. 841–844.

[10] D. Patel, R. K. Varma, R. Seethapathy, and M. Dang, "Impact of wind turbine generators on network resonance and harmonic distortion," in *Proc. 23rd Can. Conf. Elect. Comput. Eng. (CCECE)*, May 2010, pp. 1–6.

[11] *Instrument Transformers—The Use of Instrument Transformers for Power Quality Measurement*, document Rec. IEC/TR 61869-103, 2012.

[12] *Instrument transformers - Part 8: Electronic current transformers*, IEC 60044-8 (2002).

[13] M. H. J. Bollen, P. F. Ribeiro, E. O. A. Larsson, and C. M. Lundmark, "Limits for voltage distortion in the frequency range 2 to 9 kHz", *IEEE Trans. Power Del*., vol. 23, no. 3, pp. 1481–1487, Jul. 2008.

[14] K. Kunde, H. Däumling, R. Huth, H.W. Schlierf, J. Schmid, "Frequency Response of Instrument Transformers in the kHz range", *Components & Periphery* 3 Heft 6/2012, ETZ.

[15] Crotti, G. Gallo, D. Giordano, D. Landi, C. Luiso, "A Characterized Method for the Real-Time Compensation of Power System Measurement Transducers", *IEEE Trans. Instrum. Meas*., vol. 64, no. 6, pp. 1398-1405, June 2015.

[16] M. Faifer; R. Ottoboni; S. Toscani, C. Cherbaucich; P. Mazza "Metrological Characterization of a Signal Generator for the Testing of Medium-Voltage Measurement Transducers", *IEEE Trans. on Instrum. and Measur.*, Vol. 64, no: 7, July 2015, pp. 1837-1846.

[17] G. Crotti, D. Gallo, D. Giordano, C. Landi, M. Luiso and M. Modarres, "Frequency calibration of MV voltage transformer under actual waveforms," 2016 Conference on Precision Electromagnetic Measurements (CPEM 2016), Ottawa, ON, 2016, pp. 1-2

[18] W. J. M. Moore & P.N. Miljanic, "The current Comparator", IEE electrical Measurement Series 4, 1988.

[19] G. Crotti, D. Giordano, M. Modarres, D. Gallo, C. Landi and M. Luiso, "Frequency calibration of voltage transformers by digital capacitance

bridge," 2015 IEEE International Workshop on Applied Measurements for Power Systems (AMPS), Aachen, 2015, pp. 155-160.

[20] E. Mohns, J. Meisner, G. Roeissle, M. Seckelmann and M. Korejwo, "A wideband current transformer bridge," 2013 IEEE International Workshop on Applied Measurements for Power Systems (AMPS), Aachen, 2013, pp. 7-12

[21] Instrument transformers - Part 1: General requirements, IEC 61869-1:2007.

[22] E. So, "The Application Of The Current-Comparator Technique In Instrumentation And Measurement Equipment For The Calibration Of Non-Conventional Instrument Transformers With Non-Standard Rated Outputs", *IEEE Trans on Power Delivery*, Vol. 7 No. 1, January 1992, pp. 46-52.

[23] E. So, R. Arseneau and D. Bennett, "A current-comparator-based system for calibration of optical instrument transformers with analog and digital outputs," Conference Digest Conference on Precision Electromagnetic Measurements, Ottawa, Ontario, Canada, 2002, pp. 252-253

[24] http://www.ti.com/lit/ds/symlink/opa606.pdf

[25] http://www.trekinc.com/products/30-20A.asp

[26] D.Gallo, R.Langella, A.Testa, "Desynchronized Processing Technique for Harmonic and Interharmonic Analysis", *IEEE Trans. on Power Delivery*, Vol. 19, no.3, July 2004, pp. 993-1001.

[27] Crotti, G.; Gallo, D.; Giordano, D.; Landi, C.; Luiso, M.; Cherbaucich, C.; Mazza, P., "Low cost measurement equipment for the accurate calibration of voltage and current transducers," Proc. of the 2014 IEEE *Instrumentation and Measurement Technology Conference (I2MTC)*, pp.202-206, 12-15 May 2014.